Research in Astronomy and Astrophysics, 23:105006 (10pp), 2023 October https://doi.org/10.1088/1674-4527/acd52c

An Independent Degree-eight Mars Gravity Field Model and the Expected Results from the Tianwen-1 Mission

Shanhong Liu[1,2], Jianfeng Cao[1,2], Jianguo Yan[3], Hao Huang[4], Xie Li[1,2], and Jean-Pierre Barriot[5]
[1] National Key Laboratory of Science and Technology on Aerospace Flight Dynamics, Beijing 100094, China; shanhongliu@whu.edu.cn
[2] Beijing Aerospace Control Center, Beijing 100094, China
[3] State Key Laboratory of Information Engineering in Surveying, Mapping and Remote Sensing, Wuhan University, Wuhan 430079, China
[4] Department of Astronomy, Beijing Normal University, Beijing 100875, China
[5] Observatoire Géodésique de Tahiti, University of French Polynesia, F-98702 Faa'a, BP 6570 Tahiti, French Polynesia, France
Received 2022 December 21; revised 2023 April 11; accepted 2023 April 24; published 2023 September 19

Abstract

Tianwen-1 is China's first independent interplanetary exploration mission, targeting Mars, and includes orbiting, landing, and rover phases. Similar to previous Mars missions, the Tianwen-1 orbiter was designed for polar orbits during the scientific mission period but has an exceptional eccentricity of approximately 0.59. We provide the first independent eight-degree Martian gravity field model in this paper, which was developed exclusively by a team working in China with our independent software as well, based on about two months of radiometric Doppler and range data from only the Tianwen-1 mission. This model is independent from the models created by the groups at NASA Jet Propulsion Laboratory and Goddard Space Flight Center in the United States, as well as the Centre National d'Etudes Spatiales in France. Furthermore, in order to optimize the engineering and scientific benefits, we proposed a number of potential orbits for the extended Tianwen-1 mission. In order to solve a higher-degree independent Mars gravity field model, the viability of modifying the perigee height was investigated, with the priority considerations of fuel savings and implementation hazards being controlled.

Key words: gravitation – planets and satellites: fundamental parameters – methods: observational

1. Introduction

The Mars gravity field model is one of key scientific products resulting from Mars exploration. A precise gravity field model strongly affects the trajectory of the low-orbit spacecraft, and is also one of the basic tools for studying the internal structure of Mars and the mechanisms driving the evolution of the solar system. Moreover, when a Mars exploration is implemented, a model of the Mars gravity field is needed to support the orbit insertion when orbiting or landing. Precise gravity field estimation is helpful for orbit design and onboard fuel efficiency.

For this reason, the determination of a model of Martian gravity field has always played an indispensable role in the previous Mars exploration missions. Since China only implemented its first Mars exploration mission in 2020, Tianwen-1, determining an independent Mars gravity field model is still at the beginning stages. The scientific goals of Tianwen-1 mission rank Martian gravity field model estimation as important as the detection of the terrain, topography, and minerals exploration, and considered a fundamental scientific target during Chinese Mars exploration missions.

Since the 1970s, due to the continuous Mars exploration missions and their accumulation of tracking measurement data, the degree and resolution of the Martian gravity field model has been continuously improved. The inversion for the Mars gravity field model from the orbiting tracking data began with the Mariner 9 mission, where a 10×10 order and degree gravity field model was solved by Lorell et al. (1973), a 6×4 order and degree model solved by Born (1974) and a 6×6 order and degree model solved by Reasenberg et al. (1975). Later on, the Viking 1 mission entered Mars orbit in July and the Viking 2 in August of 1976. Combining the limited tracking data obtained by Mariner 9 and Viking series missions, Gapcynski et al. (1977) solved a 6×6 order gravity field model. Christensen & Balmino (1979), Balmino et al. (1982), Konopliv & Sjogren (1995) further integrated data from longer arcs to increase the solution degree to 12, 18 and 50, respectively.

In the late 1990s, the Mars Global Surveyor (MGS) and Mars Odyssey (ODY) missions were successfully implemented by NASA and unprecedentedly provided an abundant amount of data for the recovering of the Mars gravity field model. MGS was launched in 1996 December and has been in operation for nearly a decade. MGS has an almost circular orbit with an inclination of 92° and altitude of 400 km. ODY was launched in 2001 April and arrived at Mars six months later. Its orbital inclination is 93°.1 while the perigee is about 390 km and the apogee is around 455 km. Using various types of MGS tracking data, the Goddard Space Flight Center successively derived a

$75° \times 75°$ and order model MGS75B (Smith et al. 1999), an $80° \times 80°$ and order model GMM-2B and model GGM1041C of degree and order 90×90 (Lemoine et al. 2001) for the Mars gravity field model. The Jet Propulsion Laboratory (JPL) also used the same data to obtain the degree and order 75×75 models MGS75D and MGS75E (Yuan et al. 2001), and the $85° \times 85°$ and order Martian gravity field model MGS85F, MGS85F2 and MGS85H2. Konopliv et al. (2006) combined the existing MGS and ODY tracking data and solved the $95° \times 95°$ and order MGS95J Mars gravity field model.

NASA launched the Mars Reconnaissance Orbit (MRO), which is a near-circular polar satellite orbiting Mars at an altitude of about 250 km after orbit transfer. This altitude is ideally suited for collecting data to solve the Mars gravity field model at a higher degree and resolution than in the previous research. Konopliv et al. (2011) used the MGS 8 yr, the ODY 6 yr and the MRO 2 yr orbital tracking data to obtain a $110° \times 110°$ and order Martian gravity field model, MRO110B. At the same time, they also calculated the time-varying term for the low-degree coefficients in the gravity model. The collection of the longer-term tracking data has made possible the latest Martian gravity field models at a degree of 120, MRO120D (Konopliv et al. 2016) and GMM-3 (Genova et al. 2016).

The Tianwen-1 orbiter has been in operation for more than one year. At the present time, the mapping phase of the Tianwen-1 mission is about to end and the extended exploration mission will begin. The accumulated long-term orbiting tracking data may provide a new opportunity for solving independent Martian gravity field model, especially in the low-degree terms. In this paper, the current and near future status of Tianwen-1 is introduced in Section 2. In Section 3, the eight-degree Martian gravity model is determined based on the tracking data collected during the mapping phase. In Section 4, the extended mission orbits are analyzed in light of the planned and the actual progress of the Tianwen-1 mission. In Section 5, based on this analysis, we made a simulation to determine the Mars gravity field model independently to support a possible extended mission in the future.

2. Mission Status

China's first Mars mission, Tianwen-1, was successfully launched on 2020 July 23. Four mid-corrections were executed during the Earth-Mars transfer phase and the first deep space maneuver control was performed on October 9 (see Figure 1). In February 2021, Tianwen-1 braked at the perigee to begin the orbiting phase and soon the altitude of the perigee was adjusted to about 265 km. The probe has a polar orbit with large eccentricity and is similar to the MEX satellite. In 2021 May, the Tianwen-1 Mars lander successfully landed in a preselected area in the southern part of the Mars Utopia Plain. An in situ survey of Martian subsurface structure was conducted by the Zhurong rover (Li et al. 2022). At the same time, the orbiter implemented a brake at the perigee and entered an 8.2 hr relay communication orbit, followed by the mapping orbit phase.

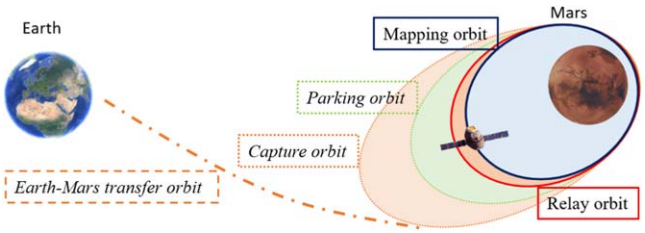

Figure 1. Tianwen-1 mission orbit view.

At this moment, Tianwen-1 has only completed mapping the Martian surface and achieved all the goals of the first phase of the mission. The orbiter however, will play a key role in extended mission. The orbital evolution of orbiter for the next eight months is plotted in Figure 2. Based on the latest status information from the Tianwen-1 orbiter, the altitude of the perigee is 210 km. It can be seen that the semimajor axis changed from 8820 to 8950 km; the eccentricity dropped from 0.596 to 0.586 but still maintains a moderate level, the height of the perigee rose from 210 to 260 km, and the orbital inclination changed from 92° to 102°. Such an orbit is different from the relay orbit and far away from the configuration of the mapping orbit. We will discuss this topic more fully in Section 5.

3. Data Reduction and New Model

3.1. Tracking Data

Processing the measurement data from the mapping phase of Tianwen-1, a first independent low degree gravity model was determined. The details are introduced as follows. The measurement data was tracked and collected by the Chinese Deep Space Network (CDSN), whose accuracy and ability was demonstrated and validated during the Chang'e missions. The CDSN is integrated with state-of-the-art technologies and includes three stations in China, one at Kashi with a 35 m antenna, one at Jiamusi with a 66 m antenna, and another one in Argentina with a 35 m antenna. During the Tianwen-1 mapping phase mission, the Jiamusi and Kashi deep space tracking stations dedicated more time on tracking and measurements than the station in Argentina, as the data for May to July of 2021 in Figure 3 show. During this time period, Tianwen-1 has simply entered the mapping mission stage and was intensively tracked by the CDSN, thus the tracking data are far less extensive than after this period.

From Figure 3, we can see the overall tracking time of Jiamusi and Kashi stations was longer than that of the overseas station. In the first week and the third week of June, the overseas station did not collect tracking data. The station in

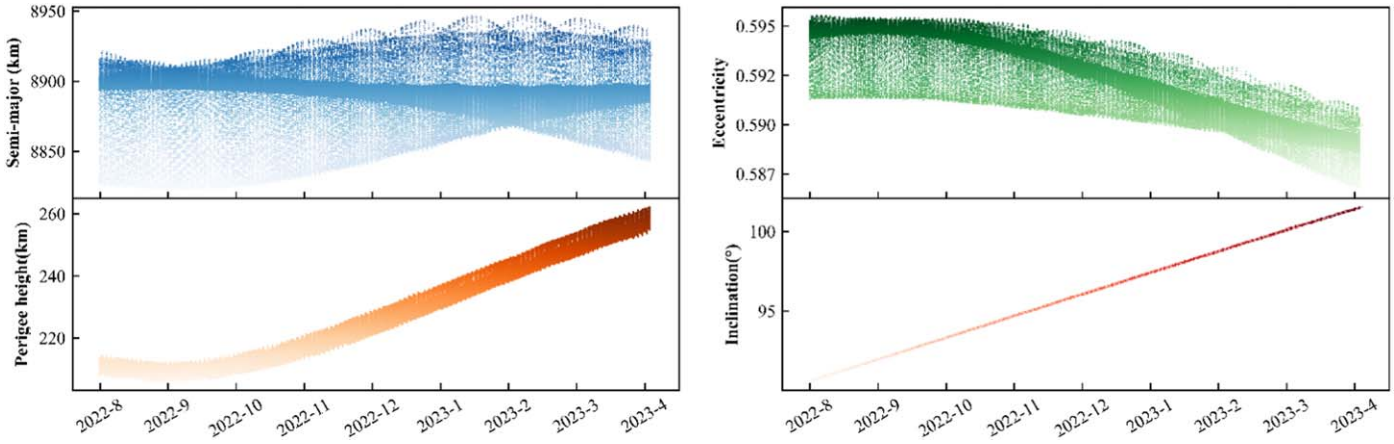

Figure 2. Orbit evolution of Tianwen-1.

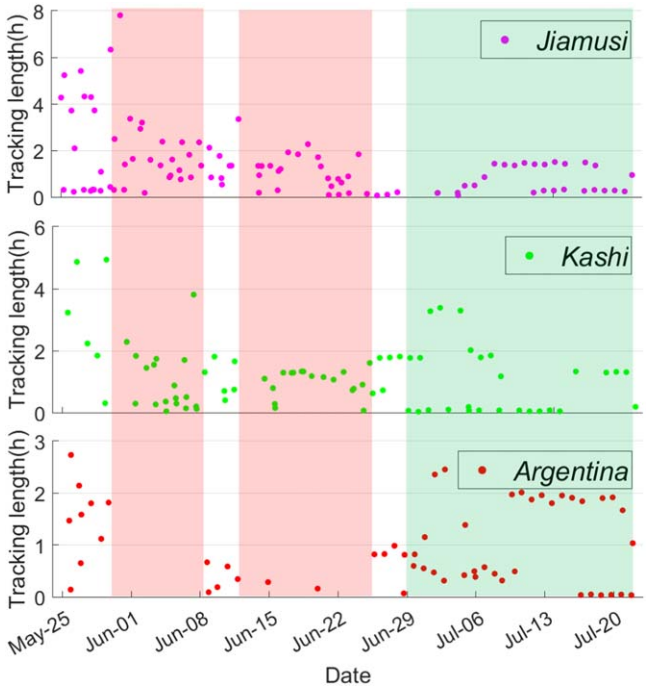

Figure 3. Tracking time statistics based on CDSN.

Argentina played a complementary role to the Jiamusi and Kashi stations although the overseas station tracking time was shorter in 2021 July. The average tracking time span of the Jiamusi, Kashi, and Argentina stations was 1.39 hr, 1.17 hr and 1.02 hr per day, respectively.

3.2. Configurations

The model parameter settings adopted in the computations and simulations are listed in Table 1. The force models for the Tianwen-1 orbiter include, the gravity field model, three-body perturbation caused by major celestial bodies in the solar system, the solar radiation pressure (SRP) perturbation, the relativistic effect, etc. The positions of the celestial bodies were provided by the JPL planetary ephemeris DE436. It should be mentioned that the water vapor radiometer installed on the China Deep Space Station helps to eliminate the tropospheric delay for the tracking data of the Tianwen-1 mission. In our POD software, the Hopfield (1963) model is used as default setting in simulation.

The data processing is described as follows. A one-day sliding period was adopted when executing precise orbit determination (POD). The POD arc was set from T to $T+80$ hr, and T represents 00:00 on one day. Due to the frequent unloading of the momentum wheel, in POD the unloading acceleration could be solved, as the orbit integration of the spacecraft is interrupted and restarted at the start and end time of the unloading. Another highlight of this work is that our new gravity field model was solved based on our in-house software (Yan et al. 2020; Liu et al. 2021, 2022), MAGREAS validated via the GEODYN-II software and Multi-satellite precision Orbit Determination and data Analysis Software in solar system (MODAS) (Cao et al. 2010).

3.3. Model Solution

Based on these configurations and the tracking data obtained from 2021 May 25 to 2021 July 22, over about two months, an eight order and degree gravity field model was solved. The C_n term coefficient and its sigma (δ_{C_n}) of our results, named Tianwen-1 Gravity Model 01 (TGM01), and the GMM-3 gravity model (marked C_n^*) are listed in Table 2. The full coefficients of our initial gravity model are recorded in Appendix A, Table A1. From Table 2, we can see that the C_n can be solved reasonably. But as the order increases, the

Table 1
Setting Parameters for POD and Gravity Recovery

Items	Types	Settings
Force model	Central mass gravity	Point mass method
	Non-Spherical gravity	GMM-3 (Genova et al. 2016)
	Atmospheric drag	Atmospheric Density Model (Stewart 1987)
	Natural satellite gravity	Phobos & Deimos
	SRP(Fixed ratio of area to mass)	Column Shadow Model, $C_r = 1.20$ (Montenbruck et al. 2002)
	N-body perturbation	Sun,planets(DE430)
	Solid tide perturbation	$k_2 = 0.169$ (Genova et al. 2016)
	Relativistic effect	Schwarzschild (Lemoine et al. 2001)
Computational benchmark	Precession Nutation Model	IAU2000/2006 precession-nutation model (Capitaine et al. 2009)
	Mars inertial system	Mars J2000.0 celestial coordinate system (Archinal et al. 2018)
	Martian fixed coordinate system	Pathfinder Mars orientation model (Konopliv et al. 2016)
Measurement correction	Station Coordinate Correction	Earth solid tide correction (Mathews et al. 1997)
	Tropospheric delay	Hopfield model (Hopfield 1963)
Data weight	Two-way/one way range rate	0.1 mm s^{-1} and 5 mm s^{-1}

Table 2
C_{n0} Parameters of this Work

n	C_{n0}	$\delta_{C_{n0}}$	C^*_{n0}(GMM-3)
2	−8.75E-04	1.85E-09	−8.75E-04
3	−1.29E-05	3.92E-09	−1.19E-05
4	4.78E-06	2.75E-09	5.13E-06
5	−5.40E-06	1.12E-08	−1.73E-06
6	1.70E-06	2.29E-09	1.35E-06
7	1.11E-06	1.12E-08	1.06E-06
8	9.71E-06	3.74E-09	1.44E-07

model coefficient difference between our model and GMM-3 increased.

Table 3 lists several typical Mars gravity field models, where the related missions and major orbital configuration information are attached. The six-order and degree gravity model obtained by Mariner 9 represents the early stage released by the United States. Later, with the following implementation of MGS, ODY and MRO missions, a relatively long period tracking data, over ten years, was be collected, and thus JPL and Goddard Space Flight Center (GSFC) greatly improved the order of the model, such as the most advanced models GMM-3 and MRO120D. Tianwen-1 has a similar orbital eccentricity with Mariner as well, but its periapse altitude is much lower.

Thus, in the future, with the accumulation of observables of Tianwen-1, an improved gravity model solution is expected. It should be pointed out that the time-varying gravity field model of Mars has increasingly become the key research over the past decade.

Overlapping arcs during an orbit period permit the evaluation of the POD accuracy and the order of Mars gravity field model. Overlaps mean that one-day arcs constrained by observations are extended by another eight hours (unconstrained) and then compared with (fully constrained) neighboring arcs. Figure 4 shows the orbit overlaps of the Tianwen-1.

Figure 4 illustrates the differences of all the overlapping arcs used in the TGM01 model recovering. The position differences of most overlapping arcs are basically less than 100 m, while the velocity differences are less than 3 cm s^{-1}. At the end of 2021 July, the difference of overlapping arcs is larger than the others indicting that the orbit determination accuracy is low, which is likely caused by the reduction of observation data on these days.

4. Extended Mission Orbits

According to Section 3, we first obtained an independent gravity field model, TGM01, by processing the two-month tracking data during the mapping phase of the Tianwen-1 orbiter. Further data collection and collation are also in progress, but the observation volume was significantly smaller in these two months. The preliminary results suggest that the outlook for further great higher degree and order gravity field model recovered during the science mapping phase is not optimistic with such an orbital structure. Actually, to recover a higher degree and order gravity field model using tracking data collected from the ground-based deep space network is related to the following factors: (a) the spacecraft orbital altitude and inclination, (b) the orbital arc length with the situation of maneuvers, (c) the tracking sampling frequency from ground-based deep space network, and (d) the accuracy of tracking measurements. For Tianwen-1, the orbital configuration and maneuvers of the orbiter are noticeable. Thus, based on the solution and experience of TGM01, the extended orbits of Tianwen-1 are worth analyzing as they were designed to solve a mid-scale degree and order gravity model.

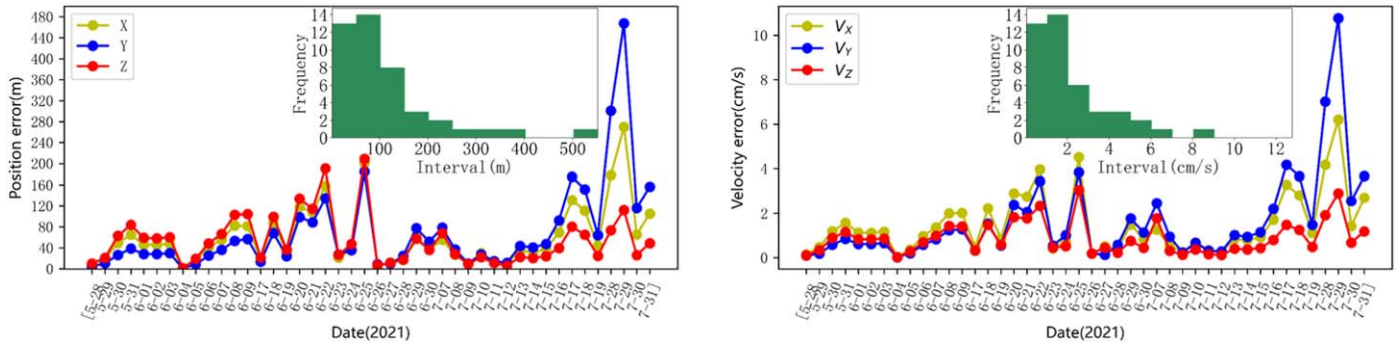

Figure 4. rms of orbit overlaps in *X*, *Y*, and *Z* directions in Mars J2000.

Table 3
Comparisons with Several Typical Models[a]

Probes	i (°)	e (°)	PA (km)	Models		
Mariner 9	∼64	∼0.6	∼1394 km	−(6 × 6, MIT, Reasenberg et al. 1975)		
MGS	∼92	∼0	∼380 km	MGS95J (95 × 95, JPL, Konopliv et al. 2006); MGGM08A (95 × 95, CNES, Marty et al. 2009)	GMM-3 (120 × 120, GSFC, Genova et al. (2016)	MRO120D (120 × 120, JPL, Konopliv et al. (2016)
ODY	∼93	∼0	∼400 km			
MRO	∼93	∼0	∼255 km			
Pathfinder	…	…	…			
VL	…	…	…			
MO	…	…	…			
Tianwen-1	∼90	∼0.6	∼265 km	TGM01(8 × 8, BACC, in this study)		

Notes. (1) *i*: Inclination, *e*: Eccentricity, PA: Periapse altitude. (2) MIT: Massachusetts Institute of Technology; JPL: NASA Jet Propulsion Laboratory; GSFC: Goddard Space Flight Center; CNES: Centre National d'Etudes Spatiales. (3) MO: MER Opportunity; VL: Viking Lander.
[a] https://solarsystem.nasa.gov/missions/

Table 4
Orbit Strategies and Adjusted Velocities

Strategy	Perigee altitude (km)	ΔV(m s^{-1})	Adjusted V_x(m s^{-1})	Adjusted V_y(m s^{-1})	Adjusted V_z(m s^{-1})
1	150	6.86117	527.375136	−688.94283	−674.07531
2	200	0.69870	530.333141	−692.78896	−677.85614
3	250	5.39531	533.258290	−696.61016	−681.59498
4	300	11.42228	536.151257	−700.38932	−685.29269

Considering the subsequent mission requirements, the Tianwen-1 orbital strategy may involve a lowering or raising the future orbital apogee altitude, as listed in Table 4. This consideration is totally different from Liu et al. (2022), which analyzed the gravity model contributions from two types of orbits, a polar and a near equatorial large eccentricity orbit, before launching Tianwen-1 mission.

As Table 4 shows, Strategy 1 focuses on lowering the orbital altitude, and strategy 2 maintains the current orbit configuration. Strategy 3 and strategy 4 are the orbit-raising schemes in response to the demands of subsequent missions. The adjusted velocities for the orbiter are also listed in Table 4.

Figure 5 shows the orbit evolution related to the four strategies. During the evolution the perigees all decrease by about 8km and then rise up. The orbital inclination shows a monotonically decreasing trend and the changes from 70° to 65°. The variation range of the eccentricity was less than 0.004.

The POD simulation period will extend from 2022 September 2 to 2023 April 2, for a total of eight months. The simulated observations include two-way range rate measurements at the Kashi, Jiamusi, and Argentina stations. The measurement noise was set to 0.1 mm s^{-1} of Gaussian white noise. We adopted the GMM-3 model truncated to degree 80 as the a priori true model. The potential coefficients at three-time

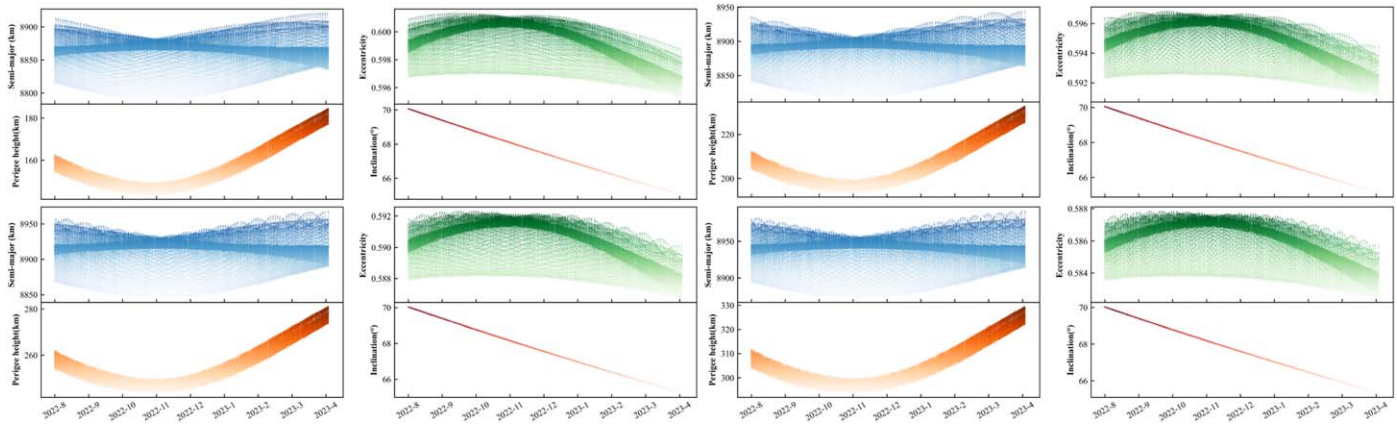

Figure 5. Orbit evolution of Tianwen-1 extended mission.

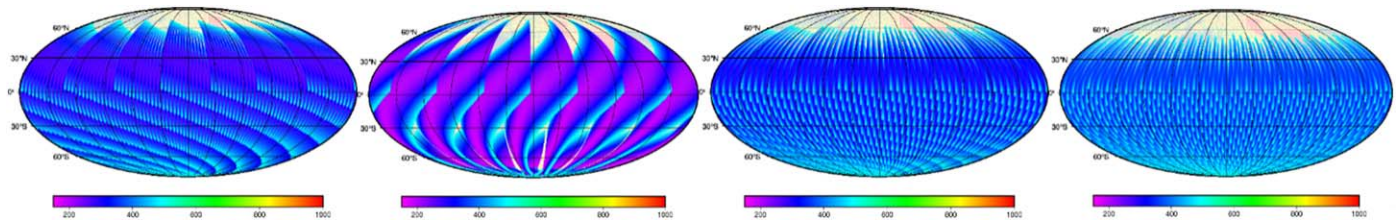

Figure 6. 6-month sub-satellite point distribution under 500 km orbital altitude. (Corresponding to strategy 1 to 4).

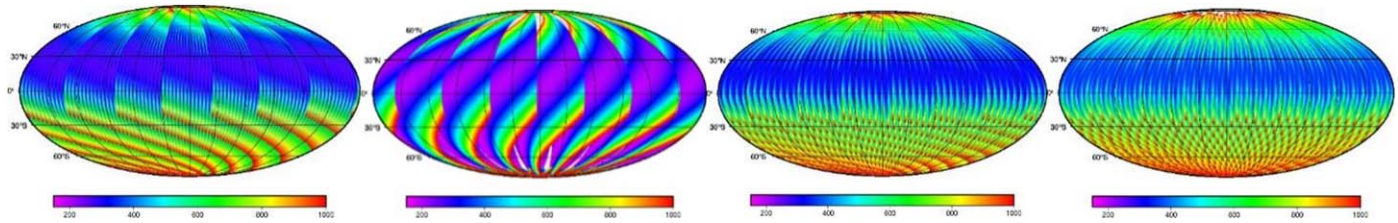

Figure 7. 8-month sub-satellite point distribution under 1000 km orbital altitude. (Corresponding to strategy 1 to 4).

Table 5
Statistics of Arc Coverage

Strategy	Coverage Time Span (hr)		Increase Percentage	
	500 km	1000 km		
1	247.24	441.85	…	…
2	266.96	453.29	7%	3%
3	224.82	430.23	−10%	−3%
4	199.43	418.44	−24%	−6%

sigma were used as the initial model for in first iteration of the gravity field model solution. The arc length was a day. The local parameters were the initial orbit elements, SRP, and measurement bias. The atmospheric drag can be ignored, because it has very small impact on such orbital configurations. The global parameters contain the degree 30 and 50 Martian gravity field model. In this simulation, the solution period was set to 3, 4, 5, 6, 7, 8 months, to find the optimal scheme and shortest observing time, separately.

5. Results and Discussion

5.1. Coverage Analysis

The sub-satellite point coverage of the extended mission orbits was analyzed. The sub-satellite points for six months and eight months was calculated from the four post-controlled orbits and the coverage conditions analyzed for the altitudes of less than 500 km and 1000 km, respectively. The results are plotted in Figures 5 and 6.

From Figure 6, it can be seen that the sub-satellite point can only cover the area south of 30°N and 60°N during the six-

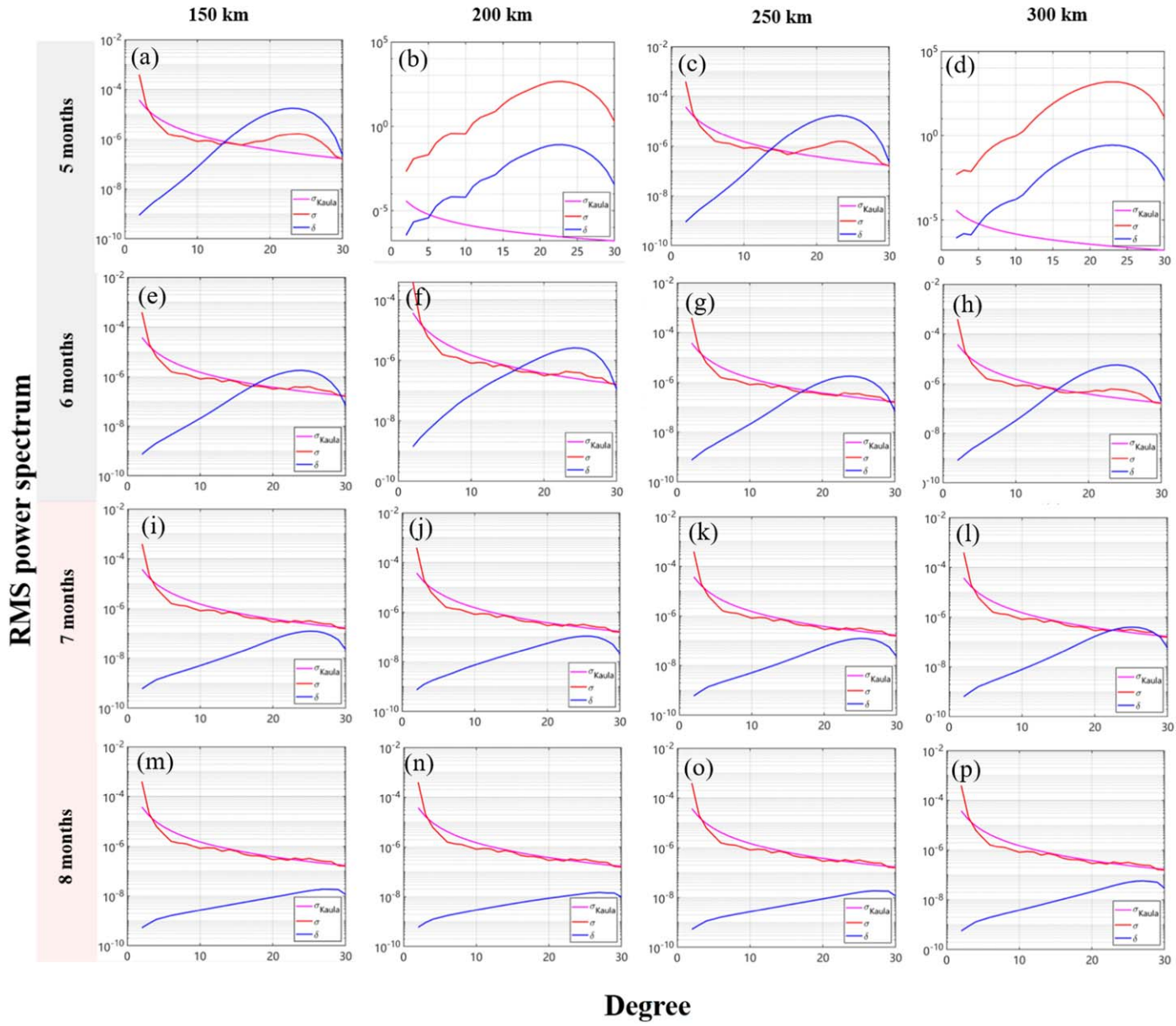

Figure 8. The power spectrum for the inversion of the 30-order gravity field model.

month period at the 500 and 1000 km altitudes. Figure 7 shows the cover area includes the south of 65°N with 500 km of the spacecraft altitude when the time span is eight months. When the height was 500 km the coverage can reach 86%, but when the height was 1000 km the coverage was about 100%. When the time span was six months, there was always a huge gap in the North Pole area.

From Figures 6 and 7, the adjustment of the spacecraft perigee altitude had significant influence on the coverage, especially in the 150 and 200 km cases. The coverage of the orbit in the 250 km case was more uniform than the 200 km case. The coverage time and percentage of increase for the arc lengths are listed in Table 5, considering the spacecraft altitude of 500 and 1000 km individually. The maximum and minimum arc lengths for the four strategies, when the perigee of the spacecraft orbit was set to 200 and 300 km are presented separately.

5.2. Power Spectrum Analysis

Power spectrum analysis of the model coefficients was applied to evaluate the validity and accuracy of the Martian gravity field model solutions, and the method details can be

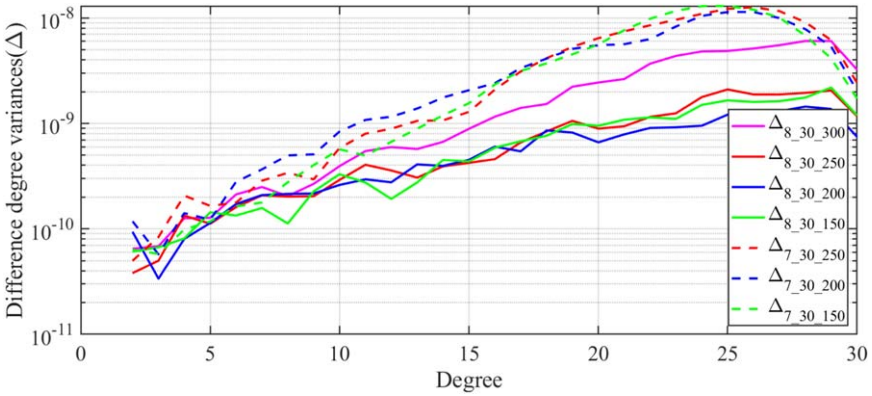

Figure 9. The covariance of 30-order gravity field model potential coefficient difference between the recovered gravity models and GMM3.

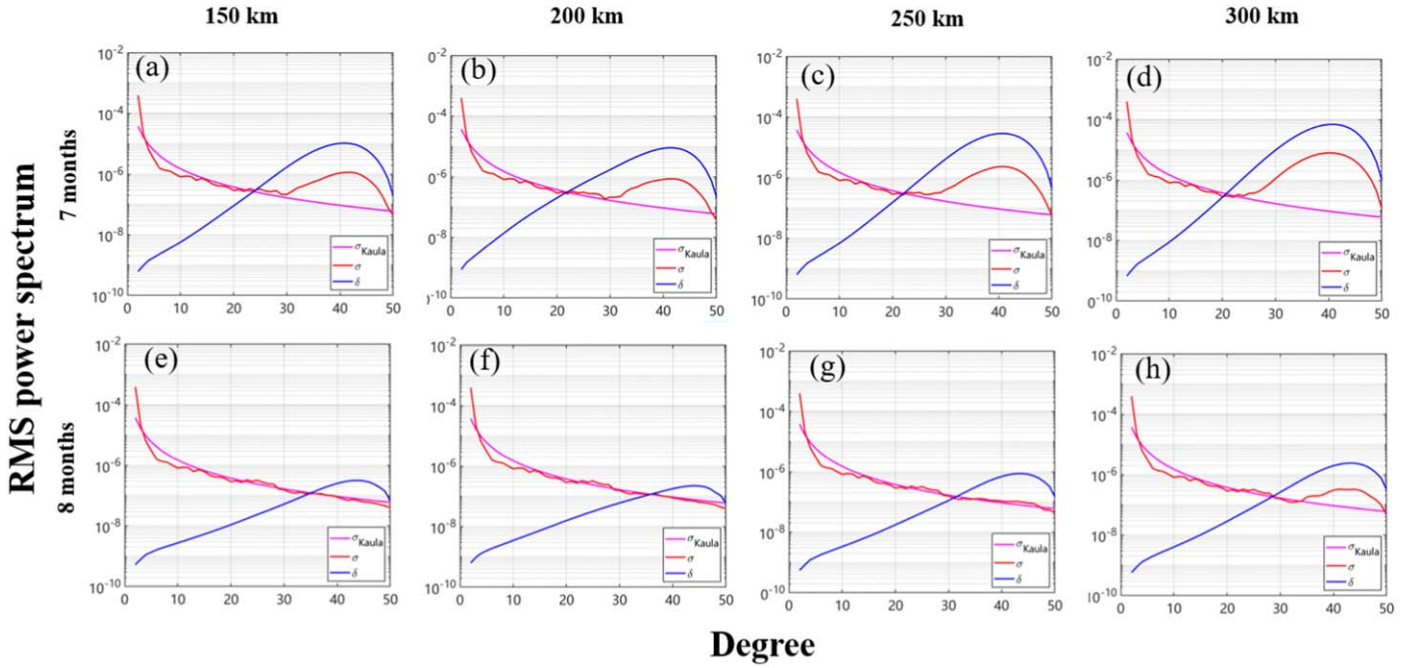

Figure 10. The power spectrum for the inversion of the 50-order gravity field model.

referred in Appendix B. The power spectrum analysis includes degree variance (σ_n) and error degree variance (δ_n).

The degree variance can be compared with the *Kaula* criterion, thus the regularized potential coefficient has zero mean value. The standard deviation is inversely proportional to the square of the degree n. For Mars, the Kuala criterion constant was taken as 1.5×10^{-4}. Figure 8 plots the coefficient degree variance (red), error degree variance (blue) and *Kaula* curve of degree 30 for each strategy.

From Figure 8, we can see that to recovery a 30-order gravity field model using depend on five or six-month Doppler data of the Tianwen-1 orbiter is impractical. For the seven-month tracking data, the recovery of the coefficients higher than order of 20 was difficult as well, except when maintaining the perigee altitude at 300 km. When the observing length was extended to eight months, the degree 30 Martian gravity field model was effectively recovered for the perigee below 300 km.

The slight difference between the feasible solutions of gravity fields was also analyzed. Figure 9 shows the difference degree variances between the recovered gravity models. Among these models, when the cumulative data was about seven months long, there was no clear differences between the 150 and 200 km perigee cases but the precision

was slightly higher than in the 250 km case. This trend is similar when the tracking span is extended to eight months, but an exception occurred when the perigee was 300 km, the accuracy of the gravity field model decreased significantly more than the degree of 10. Therefore, while accumulating measurement data, the perigee altitude should be maintained between 150 and 200 km to improve the accuracy of the degree 30 gravity field model. The ability of seven-month and eight-month accumulated data to recover a degree 50 gravity field model was also tested. The power spectrum is plotted in Figure 10.

From Figure 10, we can see that all schemes cannot recover the degree 50 gravity filed model. Figures 10(e) and (f) show that the highest order and degree coefficients can be effectively recovered to 35 degrees, indicating that these four orbital configurations still only contribute to the low or middle-order gravity field model of Mars. To sum up, a 30–35 order independent Martian gravity field model can be solved by choosing an orbital configuration below 200 km at the perigee and accumulating at least eight months of tracking data.

6. Conclusions

During the science mission phase of Tianwen-1, the orbits of the Mars capture, parking, and mapping phase were all the polar orbits with large eccentricity and a perigee altitude of about 265 km, which limited to recover Martian gravity field model. Meanwhile, the observations during tracking interval are not very abundant and the global coverage uneven. Due to frequent momentum wheel unloading, it is hard to execute POD with long arcs, and therefore, not conducive to recover the gravity field model.

In view of the implementation of the current stage of the Tianwen-1 mission, another highlight of this paper is an independent Martian gravity field solution based on several orbital configurations of the extended mission, in light of the distribution of current CDSN and tracking resources. We simulated and analyzed the solution of the Martian gravity field and its feasibility. The results show that it is possible to solve the degree 30 Martian gravity field model with at least seven months of tracking data, ideally while maintaining the perigee altitude of 150–200 km. If the conditions do not permit this height, the altitude can also be kept below 250 km. Furthermore, the gravity field can be solved using eight-month tracking data. If a higher order Martian gravity field model is needed, lowering the eccentricity might be helpful, but this depends on the status of extended Tianwen-1 mission.

Acknowledgments

This work was supported by the National Natural Science Foundation of China (NSFC) under Nos. 12203002 and 42241116, and Key Laboratory of Geospace Environment and Geodesy, Ministry of Education, Wuhan University under No. 21-01-01. J.P.B. was funded by a DAR grant in planetology from the French Space Agency (CNES).

Appendix A
Model Coefficients

The full coefficients of the gravity field model solution solved from only Tianwen-1 two-month tracking data are listed in Table A1.

Table A1
The Full Coefficients of the Degree 8 Gravity Field Model Solved from Tianwen-1

n	m	C_{nm}	S_{nm}	$\delta_{C_{nm}}$	$\delta_{S_{nm}}$
2	0	−8.75025E-04	0.00000E+00	1.84649E-09	0.00000E+00
2	1	2.50052E-09	−5.02051E-07	1.07569E-08	4.17141E-09
2	2	−7.96682E-05	4.89778E-05	1.39849E-08	4.45238E-09
3	0	−1.29430E-05	0.00000E+00	3.92444E-09	0.00000E+00
3	1	−8.42757E-06	2.77115E-05	9.32912E-09	1.67470E-08
3	2	7.17074E-06	8.69929E-06	3.33180E-08	6.93303E-09
3	3	3.50860E-05	2.55869E-05	2.12175E-09	1.33024E-09
4	0	4.78382E-06	0.00000E+00	2.75329E-09	0.00000E+00
4	1	7.87753E-07	5.10105E-06	1.37587E-08	1.49227E-08
4	2	−6.19615E-06	−8.42658E-06	2.78272E-08	7.27190E-10
4	3	1.01914E-05	7.50206E-08	2.08064E-09	2.47047E-09
4	4	7.60234E-07	−1.25626E-05	4.40339E-09	6.33153E-10
5	0	−5.40291E-06	0.00000E+00	1.11994E-08	0.00000E+00
5	1	−5.75927E-06	−2.24859E-06	3.46597E-08	1.08853E-08
5	2	−1.32526E-05	2.68733E-06	3.20281E-08	2.90280E-08
5	3	2.63215E-06	2.75347E-06	3.40250E-08	2.48273E-09
5	4	−1.32031E-05	1.12246E-06	2.90274E-08	1.25435E-08
5	5	−6.29058E-06	6.21041E-06	3.90280E-08	2.72231E-09
6	0	1.70043E-06	0.00000E+00	2.29120E-09	0.00000E+00
6	1	8.90434E-06	4.80565E-07	2.87806E-08	4.53800E-09
6	2	1.96975E-05	−1.38838E-06	5.99007E-08	3.62346E-09
6	3	2.53721E-06	1.10676E-06	4.51245E-08	1.31214E-09
6	4	3.48858E-07	6.49476E-06	3.62421E-08	3.33742E-09
6	5	2.28525E-06	2.61326E-07	9.87038E-09	1.04031E-08
6	6	2.72143E-06	4.64198E-07	4.37331E-10	1.00697E-09
7	0	1.11167E-06	0.00000E+00	1.11554E-08	0.00000E+00
7	1	1.42476E-05	6.57848E-07	3.46342E-08	3.41086E-08
7	2	−6.59765E-06	8.48042E-06	2.31235E-08	1.46669E-08
7	3	1.56411E-06	1.25272E-06	5.23523E-08	5.45361E-09
7	4	2.48193E-06	−1.36529E-05	1.03068E-08	2.36649E-08
7	5	1.08492E-07	−7.66583E-07	4.69215E-08	4.79723E-08
7	6	−1.53484E-06	−1.80483E-06	4.45722E-09	1.18250E-08
7	7	−2.75602E-06	−2.59235E-06	7.41207E-09	6.93547E-09
8	0	9.71198E-06	0.00000E+00	3.73630E-09	0.00000E+00
8	1	−5.05923E-06	−1.52617E-05	2.52351E-08	6.01693E-08
8	2	−1.77787E-05	−2.86105E-05	5.36124E-08	2.40134E-08
8	3	3.59019E-06	−7.27422E-06	2.34124E-08	6.27909E-09
8	4	1.34133E-05	−1.05027E-05	2.07405E-08	3.76821E-08
8	5	−1.00713E-05	−1.84663E-07	1.28263E-08	4.80470E-09
8	6	−4.26158E-06	−1.68686E-06	5.55508E-09	6.99862E-10
8	7	−1.05403E-05	6.33684E-06	2.30861E-08	3.41235E-09
8	8	−1.30057E-07	−8.39479E-07	3.29178E-09	6.27363E-08

Appendix B
Spherical Harmonics Theory

In order to evaluate the validity and accuracy of the Martian gravity field model, we mainly used power spectrum analysis for the gravity field coefficients. The Martian gravity field based on spherical harmonics theory can be expressed,

$$U = \frac{GM}{r}\sum_{n=2}^{N_{\max}}\sum_{m=0}^{n}(\overline{C}_{nm}\cos m\lambda + \overline{S}_{nm}\sin m\lambda) \times \overline{P}_{nm}\cos\theta\left(\frac{R}{r}\right)^n \quad \text{(B1)}$$

where R is the mean equatorial radius of the Mars reference ellipsoid, θ, λ are the colatitude and longitude of the spacecraft in the Mars geodetic coordinate system, respectively. The power spectrum analysis includes order variance and error order variance. The formula for calculating the degree variance of spherical harmonics coefficients is,

$$\sigma_n = \sqrt{\frac{\sum_{m=0}^{n}(\overline{C}_{nm}{}^2 + \overline{S}_{nm}^2)}{2\cdot n+1}} \quad \text{(B2)}$$

where $\overline{C}_{nm}$, $\overline{S}_{nm}$ are the regularized potential coefficients, n is the order, and m is the degree. The formula for calculating the error degree variance is,

$$\delta_n = \sqrt{\frac{\sum_{m=0}^{n}(\sigma_{\bar{C}_{nm}}^2 + \sigma_{\bar{S}_{nm}}^2)}{2n+1}} \quad \text{(B3)}$$

where $\sigma_{\bar{C}_{nm}}$, $\sigma_{\bar{S}_{nm}}$ are the coefficient errors.

ORCID iDs

Shanhong Liu https://orcid.org/0000-0002-2022-3389
Jianguo Yan https://orcid.org/0000-0003-2612-4776

References

Archinal, B., Acton, C., A'hearn, M., et al. 2018, CeMDA, 130, 22
Balmino, G., Moynot, B., & Vales, N. 1982, JGRB, 87, 9735
Born, G. H. 1974, JGR, 79, 4837
Cao, J., Huang, Y., Hu, X., Ma, M., & Zheng, W. 2010, ChSBu, 55, 3654
Capitaine, N., Mathews, P., Dehant, V., Wallace, P., & Lambert, S. 2009, CeMDA, 103, 179
Christensen, E. J., & Balmino, G. 1979, JGRB, 84, 7943
Gapcynski, J., Tolson, R., & Michael, W., Jr. 1977, JGR, 82, 4325
Genova, A., Goossens, S., Lemoine, F. G., et al. 2016, Icar, 272, 228
Hopfield, H. 1963, JGR, 68, 5157
Konopliv, A. S., Asmar, S. W., Folkner, W. M., et al. 2011, Icar, 211, 401
Konopliv, A. S., Park, R. S., & Folkner, W. M. 2016, Icar, 274, 253
Konopliv, A. S., & Sjogren, W. L. 1995, The JPL Mars Gravity Field, Mars50c, based upon Viking and Mariner 9 Doppler Tracking Data, Tech. Rep.9, NASA Technical Reports Server 95–5
Konopliv, A. S., Yoder, C. F., Standish, E. M., Yuan, D.-N., & Sjogren, W. L. 2006, Icar, 182, 23
Lemoine, F. G., Smith, D. E., Rowlands, D. D., et al. 2001, JGRE, 106, 23359
Li, C., Zheng, Y., Wang, X., et al. 2022, Natur, 610, 308
Liu, S., Yan, J., Cao, J., et al. 2021, E&SS, 8, e01361
Liu, S., Yan, J., Yang, X., et al. 2022, Geomatics Inf. Sci. Wuhan Univ., 48, 59
Lorell, J., Born, G. H., Christensen, E. J., et al. 1973, Icar, 18, 304
Marty, J., Balmino, G., Duron, J., et al. 2009, P&SS, 57, 350
Mathews, P., Dehant, V., & Gipson, J. M. 1997, JGRB, 102, 20469
Montenbruck, O., Gill, E., & Lutze, F. 2002, ApMRv, 55, B27
Reasenberg, R., Shapiro, I., & White, R. 1975, GeoRL, 2, 89
Smith, D. E., Sjogren, W. L., Tyler, G. L., et al. 1999, Sci, 286, 94
Stewart, J. 1987, in Estimation of Areal Evapotranspiration, 95 (Vancouver: IAHS Publ.), 227
Yan, J., Liu, S., Xiao, C., et al. 2020, A&A, 636, A45
Yuan, D.-N., Sjogren, W. L., Konopliv, A. S., & Kucinskas, A. B. 2001, JGRE, 106, 23377